ResearchOnline@JCU

JAMES COOK UNIVERSITY AUSTRALIA

This is the author-created version of the following work:

Chalak Qazani, Mohamadreza, Asadi, Houshyar, Mohamed, Shady, Lim, Chee Peng, and Nahavandi, Saeid (2022) ***A Time-Varying Weight MPC-Based Motion Cueing Algorithm for Motion Simulation Platform.*** **IEEE Transactions on Intelligent Transportation Systems, 23 (8) pp. 11767-11778.**

Access to this file is available from:

https://researchonline.jcu.edu.au/86745/

© 2021 IEEE. Personal use of this material is permitted. Permission from IEEE must be obtained for all other uses, in any current or future media, including reprinting/republishing this material for advertising or promotional purposes, creating new collective works, for resale or redistribution to servers or lists, or reuse of any copyrighted component of this work in other works.

Please refer to the original source for the final version of this work:

https://doi.org/10.1109/TITS.2021.3106970

A Time-Varying Weight MPC-Based Motion Cueing Algorithm for Motion Simulation Platform

Mohammad Reza Chalak Qazani, Houshyar Asadi, *Member, IEEE*, Shady Mohamed, Chee Peng Lim, Saied Nahavandi, *Fellow, IEEE*

***Abstract*— The motion cueing algorithm (MCA) is playing the most critical role in motion simulation platform (MSP) to reproduce the realistic motion sensation of the real car for the MSP's users while taking into cogitation of the physical boundaries of the platform. Recently, the model predictive control (MPC) is employed for designing MCAs which led to the formation of MPC-based MCAs. The purpose of the MPC-based MCA is to recalculate the optimal values of the input signals with consideration of the MSP's physical restrictions. All the current MPC-based MCAs have fix weights that can cause the conservative and inefficient utilization of the MSP's workspace limitations as they have been tuned based on the worst-case scenarios to keep the platforms within their physical limitations. Then, the error of motion sensation between the real car and MSP users increases due to the conservative utilization of the MSP's workspace boundaries. The main objective of this study is to provide more efficient workspace utilization to minimise the error of motion feeling between the real car and MSP users while respecting the workspace boundaries. A procedure according to the optimised fuzzy logic-based units is employed to calculate the appropriate MPC weights online while considering the sensed specific force error, sensed angular velocity error and the current motion status of the MSP including linear position, linear velocity and angular position of the cockpit. The proposed MPC-based MCA is designed and developed using MATLAB. The outcomes show a better motion feeling compared with the current MPC-based MCAs.**

***Index Terms*— motion cueing algorithm, time-varying weight model predictive control, fuzzy logic, multi-objective genetic algorithm, hexapod platform**

I. Introduction

THE motion simulation platforms (MSPs) are prevalent in different domains such as road safety, user training, transportation, public trust to autonomous vehicle and virtual vehicle prototyping [1-3]. The MSPs reduces the costs, time and damages while providing realistic motion sensation for the MSP users to experience virtual driving. The MSP manipulator consists of passive and active joints. The physical and dynamical boundaries of the joints cause the workspace boundaries of the MSPs [4-6]. The motion cueing algorithm (MCA) is used to reproduce the motion feeling of a real car as close as possible using the MSP with respect to the physical boundaries. The motion sickness is one of the common problems of the MSPs which happens because of the discrepancies between the motion cues and perceived visual [7]. These discrepancies happen because of limitations of the platforms and employing inefficient MCAs.

The first classical washout filter was proposed by Conrad and Schmidt [8] as the most common phase of the MCA. It consists of the high-pass and low-pass filters as well as the tilt coordination channel to produce the sustainable acceleration sensation via somatogravic illusion [9]. There are a few drawbacks using classical washout filter such as absence of the human vestibular system model and fixed parameters. Schmidt and Conrad [10] developed the adaptive washout filter to conquer the shortcomings of the classical washout filter by varying the fixed indexes of the classical washout filter. Asadi et al. [11, 12] employed the fuzzy logic to design an adaptive washout filter with consideration of both human vestibular model and physical limitations of the end-effector. Qazani et al. [13, 14] improved Asadi's [11, 12] works with consideration of the joints' limitations instead of end-effector's limitations. Recently, Qazani et al. [15] proposed the high-efficient adaptive washout filter with consideration of the dexterity to use the high dexterous area of workspace to regenerate the better high-frequency part of the motion signal. The optimal washout filter [16, 17] has the optimal structure of the classical washout filter with consideration of the human vestibular model. It aims to minimise the motion feeling error between the real car and MSP users. The most significant disadvantage of the optimal washout filter is the implementation of the white noise to extract the optimal higher order filters. Asadi et al. [18, 19] designed a genetic algorithm-based optimal washout filter to address this issue and consider the system's nonlinearities with regeneration of the motion compensator signal. Recently, Qazani et al. [20] introduced the optimal washout filter with consideration of the inverse kinematic solution to respect the joints' limitations with addition of end-effector limitations.

(*Corresponding author: Mohammad Reza Chalak Qazani*)
The authors are with the Institute for Intelligent Systems Research and Innovation, Deakin University, Geelong, VIC 3125, Australia (e-mail: m.r.chalakqazani@gmial.com; Houshyar.asadi@deakin.edu.au; shadym@deakin.edu.au; chee.lim@deakin.edu.au; saeid.nahavandi@deakin.edu.au).

The intention to obtain the optimal values of the input signals with cogitation of the workspace limitations results the first model predictive control (MPC)-based MCA by Dagdelen et al. [21]. But, their proposed MPC model could easily reach the workspace limitations because of ignoring the tilt coordination channel. Explicit MPC uses an offline computation mechanism to extract the affine functions of the whole operating regions. The computational time of the explicit MPC is lower than the traditional MPC (implicit). Then, there are suitable for MSP with low degree-of-freedom (DoF). The first explicit MPC-based MCA is proposed by Fang and Kemeny [22]. It is very fast for the MSP with a 2-DoF motion such as longitudinal. Unfortunately, the computational burden of the method increases exponentially for tackling systems with high DoFs, and it is not feasible to find the affine function in some cases. Mohammadi et al. [23] used the exponential weighting technique to increase the efficiency of the MPC-based MCA using short prediction horizon. Bruschetta et al. [24] developed a real-time MPC-based MCA for a 9-DoF MSP with real-time implementation capabilities. Mohammadi et al. [25] used the genetic algorithm with interaction of the human to optimise the weights of cost function in the MPC-based MCA. Qazani et al. [26] designed the MPC-based MCA for a midsize MSP using the decoupled model of the vestibular system to control the tilt angle more precisely. Later, Qazani et al. [27, 28] used a linear time-varying MPC-based MCA with definition of terminal conditions to consider a nonlinear kinematic model of the Hexapod manipulator, resulting in a low computational load MCA model as compared with that of NMPC [29] and lower chance of instability facing abrupt motion scenarios. Miunske et al. [29] introduced a new MPC-based MCA with consideration of the actuators' acceleration limits using inverse Jacobian matrices of acceleration kinematics. Grottoli et al. [30] conducted the first objective evaluation of MPC-based MCA using time-varying and constant reference signals.

There are two methods for evaluation of the MCA including objective and subjective studies. The objective study of the MCA has been comprehensively reviewed by Casas et al. [31]. Also, Casas et al. [32] investigated the comprehensive objective study using different MSPs with different limitations and DoFs. This assumption has been followed in lots of researches' works [21, 22, 24-30]. On the other hand, Arjoni et al. [33] used the subjective study for a flight MSP using flight operational quality assurance. Natal et al. [34] analyzed the implementation details of the classical washout filter in MSP. Pieters et al. [35] investigated the practical implementation of the classical washout filter on human control tracking behavior. Bachelder et al. [36] employed the subjective evaluation of the MCA in order to rate the workload of the pilot using flight MSP. It should be noted that the objective study of the MCA is the most fundamental part of MCA design and modification. In this research, three parameter including root mean square error (RMSE), correlation coefficient (CC) and absolute displacement of the end-effector are employed to objectively evaluate the proposed and current MPC-based MCAs.

All previous studies [21, 22, 24-27, 29-31, 37] on MPC-based MCAs including linear and nonlinear MPCs employed the fixed weight parameters. This causes to the poor utilization of the workspace as the weights are tuned for the worst-case driving scenarios to keep the cockpit within the workspace area. For instance, if the weights are tuned to use the more workspace areas, it will increase the risk of reaching to the active joints' limitations, which are the main reason for the false motion cues and motion sickness. On the other hand, the large weights lead to the poor utilization of the workspace area which can increase the motion sensation error. In this study, the fuzzy logic controllers are employed to adaptively vary the weights of the MPC model based on motion signals and cockpit positions. The variation of the MPC weighting parameters leads to regeneration of more accurate motion signals with high fidelity via a better exploitation of the workspace limitations, as compared with those of the current MPC-based MCA models with constant weighting parameters. It means that the proposed MPC-based MCA is able to generate the motion signals that can exploit larger workspace areas when the cockpit is close to the neutral position and the motion sensation error is large (i.e., by using low displacement weight). On the other hand, it is also able to better exploit the workspace constraint when the cockpit is close to the boundary limit (i.e., by using high displacement weight). In addition, a genetic algorithm (NSGA-II) is used to extract the optimal membership functions of the fuzzy controller to increase the efficiency of the proposed MPC-based MCA concerning platform workspace utilization and minimization of motion feeling error. The major objective of this study is to preferable use of the MSP workspace to minimise the motion sensation error.

Section II explains the structure of the Hexapod MSP, the MPC-based MCA with integration of the human vestibular model. The proposed fuzzy logic controller is presented in Section III to adaptively vary the weights of the MPC-based MCA. The extracted model has been developed in the Simulink environment of the MATLAB software, and results are extracted and disputed in Section IV. The conclusions are presented in Section V.

II. MPC-Based MCA For Hexapod Platform

The improvement of the hardware and software increases the utilization of the MPC as a novel control method in industries [38] because of easing the computational load of the MPC algorithm. The MPC considers the constraints of Multi-Input Multi-Output system, easily. Moreover, it can be implemented for the nonlinear model with different limitations. The MPC is a constrained optimisation technique with consideration of the limitations to reach the output signal towards the reference signal along prediction horizon N_P with implementation of the input signal along control horizon N_C. Then, the first argument of the found optimised input signal is implemented to the system (receding horizon). This process continues until the end of the motion scenario, while solving the optimisation problem at each sampling time [39].

A. Hexapod Motion Platform

The MSPs can be categorized into serial-, parallel-, and hybrid-based structure [4, 40]. Qazani et al. introduced and

investigated the regeneration of the motion cues using different MSPs such as Hexarot [41-43] and Gantry-Tau [44-46]. A Gough-Stewart platform known as Hexapod platform is a type parallel manipulator that consists of six prismatic active joints, which are attached to the base platform via six passive joints and the cockpit via six passive spherical joints as shown in Fig. 1 [47]. The cockpit regenerated the 6-DoF motion signals, which are the three linear displacements known as longitudinal, lateral and vertical along *x*-, *y*- and *z*-axis, and the three angular displacements known as *roll*-, *pitch*- and *yaw*-angle (shown as ϕ, θ and ψ). Qazani et al. [48] investigated the performance of the Gough-Stewart platform using classical and optimal washout filters

B. Human Vestibular Model

The human vestibular system consists of various components, while the main parts (otolith organs and semicircular canals) can be found in the inner ear in vestibular labyrinth. The otolith organs and semicircular canals are responsible for feeling the translational and rotational motions incorporating with linear acceleration and angular velocity motion signals [17]. The perceived translational motion signal by the real car and MSP users can be calculated as follows:

$$\mathbf{S}_F = \mathbf{a} - \mathbf{g}. \tag{1}$$

where $\mathbf{S}_F$ known as sensed specific force can be formulated in the matrix form as [19]:

$$\mathbf{S}_F = \begin{cases} f_x \triangleq a_x - g\theta \\ f_y \triangleq a_x + g\phi. \\ f_z \triangleq a_z - g \end{cases} \tag{2}$$

In this study, the Telban's vestibular model [17] which is investigated deeply by Asadi et al. [49] is applied to calculate motion sensation of the real car and MSP users. The translational motion sensed by otolith organs $\hat{f}$ is:

$$\frac{\hat{f}}{f} = K_{OTO}\left(\frac{(\tau_a s+1)}{(\tau_L s+1)(\tau_s s+1)}\right). \tag{3}$$

where τ_L are τ_s, are the long- and short-time constants of otolith organs in the longitudinal channel (τ_L=5.3 and τ_s=0.016 seconds). Also, τ_a and K_{OTO} are neural processing term lead operator and the human translational threshold unit in the longitudinal channel (τ_a=13.2 seconds and K_{OTO}=0.4). The state space matrices of the human otolith model based on Eq. (3) can be extracted using the tf2ss function in MATLAB. Also, the rotational motion sensed by semicircular canals $\hat{\theta}$ is:

$$\frac{\hat{\theta}}{\theta} = \left(\frac{\tau_1\tau_2 s^2}{(1+\tau_1 s)(1+\tau_2 s)}\right). \tag{4}$$

where τ_1 and τ_2 are the long-time constant and the adaption time constant of semicircular canals in the longitudinal channel (τ_1=5.3 and τ_2=30 seconds). It is the proposed model by Telban and Cardullo which is investigated by Asadi et al. [50]. The state space matrices of the human semicircular model based on Eq. (4) can be extracted using the tf2ss function in MATLAB.

Then, the state-space model of the vestibular system is able to be extracted by combining the Eq. (3) and Eq. (4) in the state-space mode.

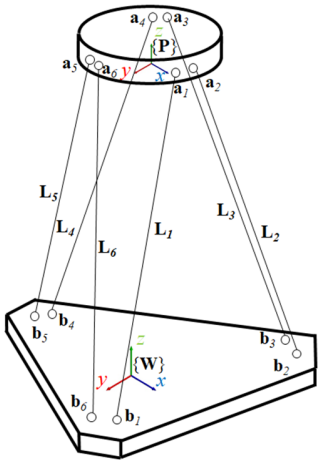


Fig. 1. The structure of the Hexapod platform.

$$\dot{\mathbf{x}}_V = \mathbf{A}_V\mathbf{x}_V + \mathbf{B}_V\mathbf{u}.$$
$$\hat{\mathbf{y}}_V = \mathbf{C}_V\mathbf{x}_V + \mathbf{D}_V\mathbf{u}. \tag{5}$$

where $\mathbf{u} = [\dot{\theta} \quad a_x]^T$ is the control action (angular velocity and linear acceleration); $\mathbf{x}_V$ is the human vestibular model state vector; while $\mathbf{A}_V$, $\mathbf{B}_V$, $\mathbf{C}_V$ and $\mathbf{D}_V$ are the state space matrices of the human vestibular model that can be found as:

$$\mathbf{A}_V = \begin{bmatrix} \mathbf{A}_{SCC} & \mathbf{0} \\ \mathbf{0} & \mathbf{A}_{OTO} \end{bmatrix}$$
$$\mathbf{B}_V = [\mathbf{B}_{SCC} \quad \mathbf{B}_{OTO}]^T$$
$$\mathbf{C}_V = \begin{bmatrix} \mathbf{C}_{SCC} & \mathbf{0} \\ \mathbf{0} & \mathbf{C}_{OTO} \end{bmatrix}$$
$$\mathbf{D}_V = [\mathbf{D}_{SCC} \quad \mathbf{D}_{OTO}]^T \tag{6}$$

where SCC and OTO indicate the semicircular system and otolith organ, respectively.

C. Model Predictive Control-based MCA

In order to extract the MPC model, the discretised state-space model of the system should be extracted to be employed inside the controller are follows:

$$\mathbf{x}_m(t+1) = \mathbf{A}_m\mathbf{x}_m(t) + \mathbf{B}_m\mathbf{u}(t).$$
$$\mathbf{y}(t) = \mathbf{C}_m\mathbf{x}_m(t) + \mathbf{D}_m\mathbf{u}(t). \tag{7}$$

where $\mathbf{A}_m$, $\mathbf{B}_m$ and $\mathbf{C}_m$ are matrices of MPC state-space model in discretised form using $T_s = 0.01\ (s)$ sampling time. As there is the linear displacement, linear velocity and angular displacement limitation cooperating with the MSP, then the state-space model of the vestibular system, which is found in Eq. (5), should be combined with the integral state-space model to respect the MSP limitations as follows:

$$\dot{\mathbf{x}}_d = \mathbf{A}_d\mathbf{x}_d + \mathbf{B}_d\mathbf{u} \tag{8}$$

where $\mathbf{A}_d$, $\mathbf{B}_d$ and $\mathbf{x}_d$ are:

$$\mathbf{A}_d = \begin{bmatrix} 0 & 1 & 0 \\ 0 & 0 & 0 \\ 0 & 0 & 0 \end{bmatrix} \tag{9}$$

$$\mathbf{B}_{\mathrm{d}} = \begin{bmatrix} 0 & 0 \\ 0 & 1 \\ 0 & 0 \end{bmatrix} \tag{10}$$

$$\mathbf{x}_{\mathrm{d}} = [\iint a_x dt^2 \quad \int \ddot{X} dt \quad \theta] \tag{11}$$

The continuous state-space model of the MPC can be extracted by combining Eq. (5) and Eq. (8). Then, it should be discretised to results Eq. (7), where $\mathbf{A}_{\mathrm{m}}$, $\mathbf{B}_{\mathrm{m}}$, $\mathbf{C}_{\mathrm{m}}$ and $\mathbf{D}_{\mathrm{m}}$ are:

$$\begin{aligned} \mathbf{A}_{\mathrm{m}} &= \begin{bmatrix} \mathbf{A}_{\mathrm{V}} & \mathbf{0} \\ \mathbf{0} & \mathbf{A}_{\mathrm{d}} \end{bmatrix} \\ \mathbf{B}_{\mathrm{m}} &= [\mathbf{B}_{\mathrm{V}} \quad \mathbf{B}_{\mathrm{d}}]^{T} \\ \mathbf{C}_{\mathrm{m}} &= \begin{bmatrix} \mathbf{C}_{\mathrm{V}} & \mathbf{0} \\ \mathbf{0} & \mathbf{I} \end{bmatrix} \\ \mathbf{D}_{\mathrm{V}} &= [\mathbf{D}_{\mathrm{V}} \quad \mathbf{0}]^{T} \end{aligned} \tag{12}$$

where $\mathbf{I}$ and $\mathbf{0}$ are identity and zero matrices. As such, the state vector of Eq. (6) is $\mathbf{x}_{\mathrm{m}} = [\mathbf{x}_{\mathrm{V}} \quad \mathbf{x}_{\mathrm{d}}]^{T}$.

There are limitations on the rate of input, input and output. Then, the rate of the states and inputs should be extracted as $\Delta\mathbf{x}_{\mathrm{m}}(t) \triangleq \mathbf{x}_{\mathrm{m}}(t) - \mathbf{x}_{\mathrm{m}}(t-1)$ and as $\Delta\mathbf{u}(t) \triangleq \mathbf{u}(t) - \mathbf{u}(t-1)$. The augment state-space model can be defined as:

$$\begin{aligned} \mathbf{x}(t+1) &= \begin{bmatrix} \mathbf{A_m} & \mathbf{0} \\ \mathbf{C_m A_m} & \mathbf{I} \end{bmatrix} \mathbf{x}(t) + \begin{bmatrix} \mathbf{B_m} \\ \mathbf{C_m B_m} \end{bmatrix} \Delta\mathbf{u}(t). \\ \mathbf{y}(t) &= [\mathbf{0} \quad \mathbf{I}]\mathbf{x}(t) \end{aligned} \tag{13}$$

where rate of the input $\Delta\mathbf{u}$ and $\mathbf{x}(t) \triangleq \begin{bmatrix} \Delta\mathbf{x_m}(t) \\ \mathbf{y}(t) \end{bmatrix}$ are the control input and state vector of the new generated model in Eq. (13).

The matrices of the new model in Eq. (13) are shown as $\mathbf{A}$, $\mathbf{B}$ and $\mathbf{C}$. Then, the new state-space model in Eq. (13) can be extracted as follows:

$$\begin{aligned} \mathbf{x}(t+1) &= \mathbf{A}\mathbf{x}(t) + \mathbf{B}\Delta\mathbf{u}(t). \\ \mathbf{y}(t) &= \mathbf{C}\mathbf{x}(t) \end{aligned} \tag{14}$$

The aim of the MPC is to compute and estimate the future output in a prediction horizon N_P with implementation of the control action in the control horizon N_C. The prediction of the states and outputs in the n sample time can be calculated as

$$\begin{aligned} \mathbf{x}(t+1|t) &= \mathbf{A}\mathbf{x}(t) + \mathbf{B}\Delta\mathbf{u}(t). \\ \mathbf{y}(t+1|t) &= \mathbf{C}\mathbf{A}\mathbf{x}(t) + \mathbf{C}\mathbf{B}\Delta\mathbf{u}(t) \\ &\cdots \\ \mathbf{x}(t+N_P|t) &= \mathbf{A}^{N_P}\mathbf{x}(t) + \mathbf{A}^{N_P-1}\mathbf{B}\Delta\mathbf{u}(t) + \mathbf{A}^{N_P-2}\mathbf{B}\Delta\mathbf{u}(t+1) + \cdots + \mathbf{A}^{N_P-N_C}\mathbf{B}\Delta\mathbf{u}(t+N_c-1) \\ \mathbf{y}(t+N_P|t) &= \mathbf{C}\mathbf{A}^{N_P}\mathbf{x}(t) + \mathbf{C}\mathbf{A}^{N_P-1}\mathbf{B}\Delta\mathbf{u}(t) + \mathbf{C}\mathbf{A}^{N_P-2}\mathbf{B}\Delta\mathbf{u}(t+1) + \cdots + \mathbf{C}\mathbf{A}^{N_P-N_C}\mathbf{B}\Delta\mathbf{u}(t+N_c-1) \end{aligned} \tag{15}$$

where $x(t+n|t)$ are the sample time of the control and the state in the n sample time.

The new vector form of inputs and outputs of Eq. (15) called $\Delta\mathbf{U}$ and $\mathbf{Y}$ where $\Delta\mathbf{U} \in \mathbb{R}^{(N_C \cdot N_{in}) \times 1}$ and $\mathbf{Y} \in \mathbb{R}^{(N_P \cdot N_{out}) \times 1}$. N_{in} and N_{out} are the size of $\Delta\mathbf{u}$ and $\mathbf{y}$, respectively. Then, the input-output evaluation of the model can be presented as follows:

$$\mathbf{Y} = \mathbf{f} + \mathbf{G}\Delta\mathbf{U} \tag{16}$$

where $\mathbf{f}$ and $\mathbf{G}$ are matrices as follows:

$$\mathbf{f} = \begin{bmatrix} \mathbf{CA} \\ \mathbf{CA^2} \\ \vdots \\ \mathbf{CA}^{N_P} \end{bmatrix} \mathbf{x}(t)$$

$$\mathbf{G} = \begin{bmatrix} \mathbf{CB} & \mathbf{0} & \cdots & \mathbf{0} \\ \mathbf{CAB} & \mathbf{CB} & \cdots & \mathbf{0} \\ \vdots & \vdots & \ddots & \vdots \\ \mathbf{CA}^{N_P-1}\mathbf{B} & \mathbf{CA}^{N_P-2}\mathbf{B} & \cdots & \mathbf{CA}^{N_P-N_C}\mathbf{B} \end{bmatrix} \tag{17}$$

The definition of the reference signal, $\mathbf{R}_{\mathrm{ref}}$, is critical to obtain the cost function. There are two hypotheses to define the reference signal including time-invariant and time-varying methods. In this work, the time-invariant method is selected to decrease the sensitivity of the system to the sudden changes in the motion signal. The cost function, $\mathbf{J}$ is defined to decrease the motion sensation error between the real car and MSP users, as follows:

$$\mathbf{J}(\Delta\mathbf{U}) = (\mathbf{R}_{\mathrm{ref}} - \mathbf{Y})^{\mathrm{T}}\mathbf{Q}(\mathbf{R}_{\mathrm{ref}} - \mathbf{Y}) + \mathbf{U}^{\mathbf{T}}\mathbf{S}\mathbf{U} + \Delta\mathbf{U}^{\mathrm{T}}\mathbf{R}\Delta\mathbf{U} \tag{18}$$

where $\mathbf{Q}$, $\mathbf{S}$ and $\mathbf{R}$ are the weighting matrices of the output, input and rate of input, respectively. In the proposed method, the weights of the outputs, $\mathbf{Q}$ are time-varying and should be recalculated online at each time step. The $\mathbf{S}$ and $\mathbf{R}$ weighting matrices are fixed, owing to the ability to monitor the parameters (through sensors) in weighting matrix $\mathbf{Q}$ and the ability of the MSP to regenerate large acceleration signals using parallel MSP structures. Also, The MSP user motion sensation is also being monitored using mathematical model of motion vestibular system.

The input arrangement $\mathbf{U}$ can be found based on $\Delta\mathbf{U}$ and $\mathbf{u}(t-1)$ as follows:

$$\mathbf{U} = \underbrace{\begin{bmatrix} \mathbf{I} & \mathbf{0} & \cdots & \mathbf{0} \\ \mathbf{I} & \mathbf{I} & \cdots & \mathbf{0} \\ \vdots & \vdots & \ddots & \vdots \\ \mathbf{I} & \mathbf{I} & \cdots & \mathbf{I} \end{bmatrix}}_{\mathbf{T}} \Delta\mathbf{U} + \underbrace{\begin{bmatrix} \mathbf{u}(t-1) \\ \mathbf{u}(t-1) \\ \vdots \\ \mathbf{u}(t-1) \end{bmatrix}}_{\bar{\mathbf{U}}_i} \tag{19}$$

The new cost function can be found by substituting the Eq. (16) and Eq. (19) in Eq. (18) as:

$$\begin{aligned} \mathbf{J}(\Delta\mathbf{U}) = (\mathbf{R}_{\mathrm{ref}} - \mathbf{f} - \mathbf{G}\Delta\mathbf{U})^{\mathrm{T}}\mathbf{Q}(\mathbf{R}_{\mathrm{ref}} - \mathbf{f} - \mathbf{G}\Delta\mathbf{U}) + \\ (\mathbf{T}\Delta\mathbf{U} + \bar{\mathbf{U}}_i)^{\mathbf{T}}\mathbf{S}(\mathbf{T}\Delta\mathbf{U} + \bar{\mathbf{U}}_i) + \Delta\mathbf{U}^{\mathrm{T}}\mathbf{R}\Delta\mathbf{U} \end{aligned} \tag{20}$$

with a definition of the $\mathbf{H} \triangleq 2(\mathbf{G}^{\mathrm{T}}\mathbf{Q}\mathbf{G} + \mathbf{R} + \mathbf{T}^{\mathrm{T}}\mathbf{S}\mathbf{T})$ and $\mathbf{g} = 2(\mathbf{G}^{\mathrm{T}}\mathbf{Q}(\mathbf{f} - \mathbf{R}_{\mathrm{s}}) + \mathbf{T}^{\mathrm{T}}\mathbf{S}\bar{\mathbf{U}}_i)$, the Eq. (20) can be extracted as:

$$\mathbf{J}(\Delta\mathbf{U}) = \tfrac{1}{2}\Delta\mathbf{U}^{\mathrm{T}}\mathbf{H}\Delta\mathbf{U} + \Delta\mathbf{U}^{\mathrm{T}}\mathbf{g} \tag{21}$$

It should be noted that using time-varying weight MPC needs to update the Hessian matrix $\mathbf{H}$ and gradient matrix $\mathbf{g}$ should be updated at each time-step according to the calculated weight matrix $\mathbf{Q}$ via FIC units. Also, the MPC horizons including prediction and control horizons are chosen based on the conducted research by Mohammadi et al. [51], which aim to ease the computational load due to the calculation of the Hessian and gradient matrices. Qazani et al. [52] employed a butterfly optimization algorithm to extract the optimal MPC

horizons in order to ease the computational load as well as decreasing the motion sensation error between he MSP's user and the real vehicle's driver. When combined with linear constraints, it is the classical expression of the QP problem that is used to optimise the $\Delta\mathbf{U}$. Then, the constraints of the MPC model should be formulated as a function of $\Delta\mathbf{U}$ as $(\mathbf{Ax} < \mathbf{b})$ to calculate an analogous formulation. It is presented as:

$$\begin{bmatrix}\mathbf{M}_1\\ \mathbf{M}_2\\ \mathbf{M}_3\end{bmatrix}\Delta\mathbf{U} \leq \begin{bmatrix}\mathbf{n}_1\\ \mathbf{n}_2\\ \mathbf{n}_3\end{bmatrix} \tag{22}$$

The constraints are interpreted into three groups, such as limitations on the outputs, inputs and inputs rates. $\mathbf{M}_1$ and $\mathbf{n}_1$ matrices are related to the limitations of the input rates, which are the angular acceleration $\ddot{\theta}$ and linear jerk, $Jerk_x$ of the hexapod MSP. $\mathbf{M}_2$ and $\mathbf{n}_2$ are defined as the constraint matrices of the input, which are the angular velocity $\dot{\theta}$ and linear acceleration a_x of the hexapod MSP. $\mathbf{M}_3$ and $\mathbf{n}_3$ are related to the output results, which are the linear displacement x, linear velocity V_x, and angular displacement θ. These parameters are presented in Table I. With the definition of matrices in Eq. (22), Eq. (18) can be reshaped in a QP problem.

III. Fuzzy Logic Controller

A. Fuzzy Logic

The theory of fuzzy logic into the area of the application and intelligent system are introduced by Yager and Zadeh [53]. The fuzzy logic provides reliable results in an application with a highly stochastic and uncertain inputs system [54, 55]. The fuzzy logic is employed in MCA because they handle uncertain and stochastic input easily [11, 12]. As one of the main MPC-based MCA's problems is related to the constant weights, the variation of the output weights $\mathbf{Q}$ based on the applied motion signals and the current position of the MSP can ensure better performance and more accurate driving motion sensation for all the situations while respecting the platform's limitations.

B. Proposed Fuzzy Logic Controller

The schematic structure of the proposed MPC-based MCA using fuzzy logic to adaptively change the weights of the MPC is presented in Fig. 2(a). Fig. 2(b) presents a schematic structure of the compensator unit, which is employed to update the fuzzy control action according to the current situation of the cockpit. The MSP user generates the realistic motion signal, denoted as $\{\dot{\theta}, a_x\}_v$, by pushing the gaze or brake pedal or turning the steering wheel based on his/her visual information in the simulated environment. The generated vehicle motion signal is employed in the human vestibular model based on Eq. (5) to compute the sensed angular velocity $\hat{\theta}$ and sensed specific force $\hat{f}$. The resulting motion sensation signal is used as an MPC reference signal. In addition, the MPC model computes the optimal input signal, denoted as $\{\dot{\theta}, a_x\}_s$, to provide the realistic motion sensation for the MSP user (as if it is from a real vehicle) along prediction horizon. This implementation is straightforward in all MPC models. There are five weighting

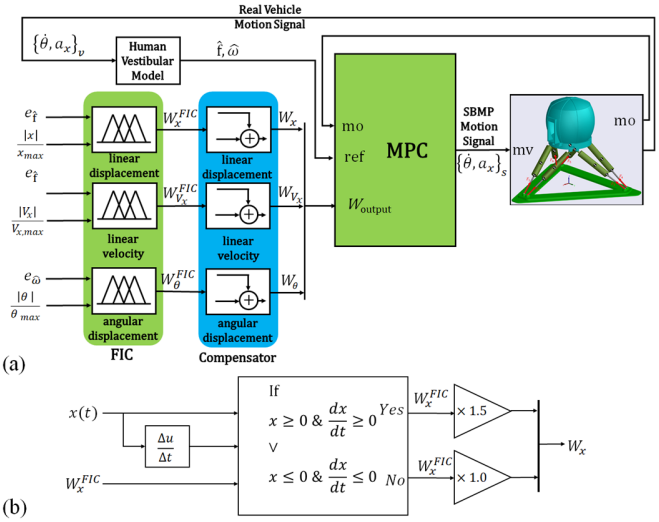


Fig. 2. (a): The schematic structure of the proposed MPC-based MCA using fuzzy logic controller blocks; (b): The schematic structure of the compensator unit.

parameters in an MPC-based MCA, namely the sensed specific force, sensed angular velocity, linear displacement, linear velocity, and angular displacement. In this study, these weighting parameters are of a time-varying nature, in order to increase the efficiency of the proposed method. Nevertheless, the motion sensation weights are fixed because they are not constrained by the workspace limitations. Therefore, the three fuzzy logic blocks are used to produce the appropriate weights of the MPC for the linear displacement, W_x, linear velocity W_{V_x} and angular displacement W_θ using the position information of the MSP for different driving inputs.

It is highly recommended to stop the MSP from reaching the workspace limitations. If the MSP reaches the workspace limitation, the controller unit of the manipulator will saturate the input signals to restrict the active joints inside the physical constraints. This leads the artefact or consequently, motion feeling error between the real car and MSP users. The input signals of the fuzzy blocks should be normalised before applying to the fuzzy units. The first inputs of the first fuzzy block are the translational and rotational error of sensed motions between the real car and MSP users. The input signal is divided to five units as very positive, positive, zero, negative and very negative to normalise the motion sensation errors between the real car and MSP users. The human vestibular system of the human body cannot perceive the exact quantity of the motion while it can distinguish if the motion is very big or big or small with motion direction. For this reason, the motion sensation error of the rotational and translational is categorised in five groups, including very negative, negative, zero, positive

TABLE I
THE WORKSPACE BOUNDARIES OF THE HEXAPOD PLATFORM IN THE LONGITUDINAL CHANNEL

Index	Position	Velocity	Acceleration
x-axis	±0.1 m	±15 m/s	±35 m/s^2
Pitch-angle	±0.0872 rad	±2.35 rad /s	±43.63 rad /s^2

and very positive as shown in Fig. 3. The significant difference between the membership functions of the rotational and translational error inputs is due to the structure of the human otolith organs and semicircular canals [17]. The dead zone on the membership functions of the rotational error is due to the human threshold unit as MSP's user is not supposed to sense the angular motion [12].

Fig. 4 shows the membership functions of the second input, known as the position of the MSP. The inputs of the linear displacement, linear velocity and angular displacement are normalised by dividing to the boundaries of the MSP in the Cartesian coordinate system. It is also divided into five membership functions as very near, near, middle, far and very far from the neutral position according to the current position of the MSP. The output membership function of the fuzzy block is shown in Fig. 5, which are divided into five cases as very small, small, medium, big and very big.

There are various shapes of membership functions such as triangular, trapezoidal, Gaussian, and sigmoid for different purposes. However, the triangular membership functions are employed in this study because they have a lighter computational load. Also, they can be defined with a small amount of data, and they can be specified in the asymmetric form. The membership functions are overlapping, which means the inputs and output have their membership functions from the overlapped membership functions as presented in Fig. 3-5. To determine the membership functions of the fuzzy blocks the nine parameters known as $d_{\hat{f}_x}$, $d_{\hat{f}_{V_x}}$, $d_{\hat{\omega}_\theta}$, d_x, d_{V_x}, d_θ, d_{W_x}, $d_{W_{V_x}}$ and d_{W_θ} should be specified as presented in Fig. 3-5, respectively.

The rules of the fuzzy logic are defined based on Mamdani-type fuzzy as shown in Table II which uses the position of the MSP and motion sensation error as the inputs. The control output produces according to the fuzzy rules. For instance, if the distance of the cockpit from the neutral position is very near and the error of sensed specific force between the real car and MSP users is very positive, the weight of the linear displacement should be very small to less penalize the linear displacement of the MSP. Note that, if the distance of the cockpit from the neutral position is very far and the error of sensed specific force is near zero, there is a need of very big weight of the linear displacement. In Addition, if the cockpit is situated very far from neutral position and the sensation error is very positive or very negative, the controller should produce high value for the weight of linear displacement. The motion sensation errors (sensed rotational or translational motion) changes the output when it is very negative or positive. Fig. 6 presents the characteristic surface of the proposed fuzzy controller with predefined fuzzy rules.

As tuning these parameters manually is a suboptimal process, the multi-objective genetic algorithm (NSGA-II [56, 57]) is employed to find the optimum value of these nine parameters, which are shown in Fig. 3-5. The sub-cost functions are the error of the sensed angular velocity and sensed specific force (objective 1) between the real car and MSP users and the linear displacement, linear velocity and angular velocity of the MSP (objective 2). Then, the cost functions J_{MCA1} and J_{MCA2} are defined as an integration on the quadratic form of the inputs,

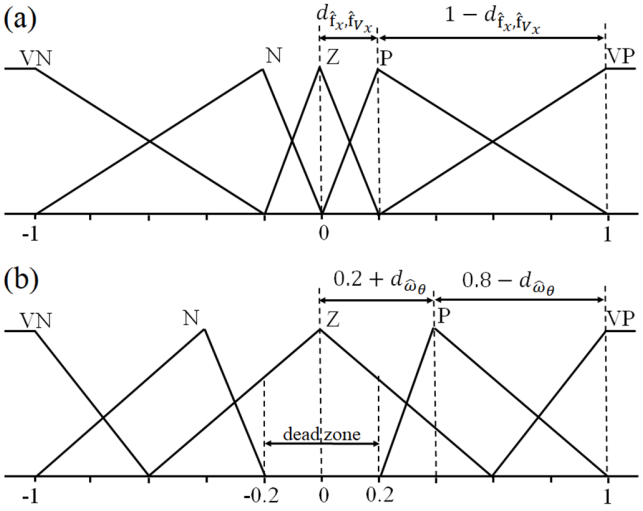


Fig. 3. The membership functions: (a) translational sensation error; (b)rotational sensation error.

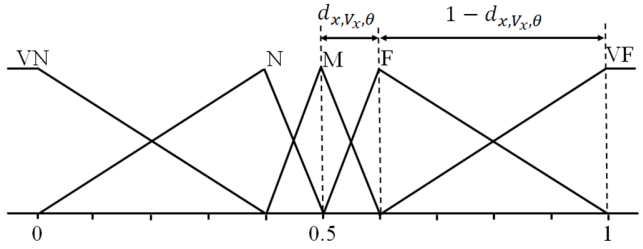


Fig. 4. The membership functions of the linear displacement, linear velocity and angular displacement inputs.

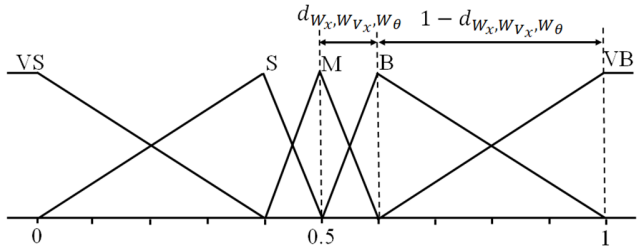


Fig. 5. The membership functions of linear displacement, linear velocity and angular position weights fuzzy outputs.

TABLE II
FUZZY CONTROL RULES FOR LINEAR DISPLACEMENT WEIGHT PARAMETER TUNING

W_x		$e_{\hat{f}}$				
		VN	N	Z	P	VP
$\frac{\lvert x\rvert}{x_{max}}$	VN	VS	VS	VS	VS	VS
	N	VS	S	S	S	VS
	M	S	M	M	M	S
	F	M	B	B	B	M
	VF	B	VB	VB	VB	B

VN: very negative and very near; N: negative and near; Z: zero; P: positive; VP: very positive; M: middle and medium; F: far; VF: very far; VS: very small; S: small; B: big; VB: very big.

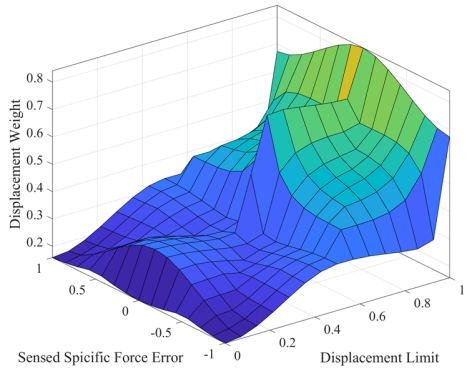


Fig. 6. The surface of the fuzzy controller based on predefined fuzzy rules.

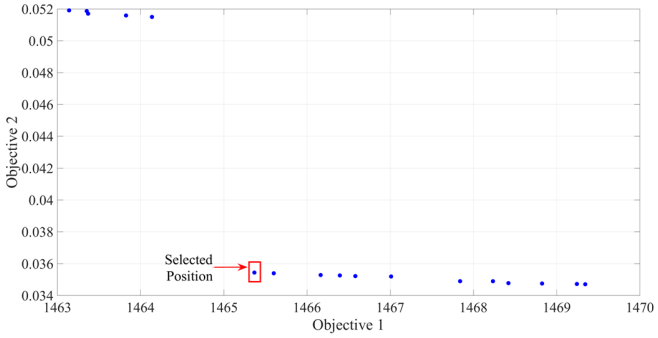


Fig. 7. Pareto-front of the Multi-objective genetic algorithm.

input rates and outputs as extracted in Eq. (16) as:

$$J_{MCA1} = w_{\hat{f}_x} \int (\hat{f}_x - f_x) dt + w_{\hat{\omega}_\theta} \int (\hat{\omega}_\theta - \omega_\theta) dt \quad (23)$$

$$J_{MCA2} = w_x \int x^2 dt + w_{V_x} \int {V_x}^2 dt + w_\theta \int \theta^2 dt \quad (24)$$

where $w_{\hat{f}_x} = 400$, $w_{\hat{\omega}_\theta} = 1$, $w_x = 1$, $w_{V_x} = 0.0667$ and $w_\theta = 0.667$ are the weighting factors of the sensed specific force, sensed angular velocity, linear displacement, linear velocity, and angular displacement of the MPC-based MCA, respectively. They can be determined by trial-and-error and using expert knowledge of the system, which act as appropriate factors for the cost functions with respect to the MSP workspace limitations shown in Table I.

The initial parameters of the multi-objective genetic algorithm should be selected appropriately to increase the convergence speed and accuracy of the solution. In this research, the high crossover fraction and a low mutation rate are selected based on the recommended settings by De Jong and Michell [58, 59]. The guideline is used in many studies [1, 11, 60]. Table III shows the adjustments of the multi-objective genetic algorithm. The population size of the study is 104. The obtained results of the multi-objective genetic algorithm demonstrate that the appropriate parameters have been chosen (mutation rate, crossover friction, and population). Fig. 7 shows the non-dominated Pareto-front for the multi-objective genetic algorithm, which is mapped into two cost functions (error of motion sensation and displacement). Keeping the MSP inside the workspace limitations and respecting the maximum error of the sensed angular velocity under the human threshold are the requirements of the solution. If the solution does not satisfy the requirement (workspace limitations and maximum error of sensed angular velocity), it will be rejected and substituted by another chromosome. The optimised triangular membership functions of the fuzzy set using multi-objective genetic algorithm are presented in Table IV. It should be noted that a series of motion scenarios combined with white noises are used in the tuning process of the FIC membership functions in order to increase the homogeneity of the proposed method. In order to evaluate the performance of the NSGA-II, the statistical t-test has been established using the significance level of 0.05 and 18 runs . The results show that the two-tailed p-values of J_{MCA1} (Eq. (23)) and J_{MCA2} (Eq. (24)) are less than 0.0001. It proves the extremely statistically significant of the NSGA-II. Besides, the confidence interval of these two groups are 95%.

The fuzzy unit will not be able to improve the performance of the MPC-based MCA, solely. There is a need for a compensator unit to show the tremendous beneficial points of the MPC-based MCA using fuzzy logic-based adaptive weight tuning. The fuzzy unit is very stiff especially when the cockpit is close to the workspace limitations. The employment of the compensator enhances the fuzzy unit to produce more proper control action based on the situation of the motion scenario.

C. *Compensator Unit*

To give the developed fuzzy unit the ability to consider the MSP's motion information, designing the compensator unit is necessary. The compensator unit which is shown in Fig. 2.b is added to the fuzzy units to update the weights according to the current motion status of the MSP including its distance from physical limitations as well as the direction of the motion. The fuzzy unit increases the weights of the outputs when the MSP is close to the platform's limitations in order to prevent hitting the limitations. On the other hand, the MSP sometimes can get close to the workspace boundaries and turn back to the neutral positions according to the motion signals. The current MPC-based MCA with the constant output weights provides better

TABLE III
MULTI-OBJECTIVE TUNING PARAMETERS

Parameters	Value
Variables	$[d_{\hat{f},x}; d_{\hat{f},V_x}; d_{\hat{\omega}}; d_x; d_{V_x}; d_\theta; d_{W_x}; d_{W_{V_x}}; d_{W_\theta}]$
Population size	104
Maximum Generation	45
Upper limit	[1; 1; 0.8; 0.5; 0.5; 0.5; 0.5; 0.5; 0.5]
Lower limit	[0; 0; 0.2; 0; 0; 0; 0; 0; 0]
Mutation function	Adaptive Feasible
Crossover rate	0.8
Tolerance	10^{-6}

TABLE IV
PARAMETERS OF THE MEMBERSHIP FUNCTIONS

Parameters	Value
$d_{\hat{f},x}; d_{\hat{f},V_x}, d_{\hat{\omega}_\theta}$	[0.0102; 0.2151; 0.6070]
d_x, d_{V_x}, d_θ	[0.4771; 0.1874; 1258]
$d_{W_x}, d_{W_{V_x}}, d_{W_\theta}$	[0.0141; 0.2828; 0.2255]

results compared to the proposed MPC-based MCA in this situation. The compensator unit should monitor the position and direction of the cockpit to add the compensated value to increase the effectiveness of the proposed model compared to the current MPC-based MCA. For instance, if the cockpit is situated in the positive side of the *x*-axis, while it is surging towards the positive side of the *x*-axis, the compensator unit will increase the weight of the linear displacement in order to prevent the cockpit reaching the workspace boundaries of linear displacement. On the other hand, if the cockpit is in the positive side of the *x*-axis and it is moving towards the negative side of *x*-axis, the extracted weights of the fuzzy unit are not changed via compensator unit because the cockpit is moving toward the neutral position. The same strategy is employed when the cockpit is located on the negative side of the *x*-axis. The effectiveness of the fuzzy logic block increases dramatically while the compensator unit is added.

IV. Result and Discussion

The proposed model of the MPC-based MCA in Section II and Section III is modelled in MATLAB software. In addition, the classical washout filter introduced by Conrad and Schmidt [8] and the current MPC-based MCA using constant weighting parameters introduced by Bruschetta et al. [24] are modelled in MATLAB for performance comparison with the proposed method. The MCA regenerates the motion signals to make the motion sensation realistic for the MSP user. The MPC has a low computational load, as the KWIK algorithm [61] is used to solve the quadratic formulation of the MPC. The model can run in a real-time mode, with 0.01s as the time step, to yield reasonably fast results. Therefore, we have run the model in a real-time mode with 0.01 (s) as a time step to have a sync model with the platform and to reach reasonable results. To tune the MPC model with and without using fuzzy logic, the prediction and control horizons are initially tuned with consideration of the real-time solution of the model. Then, the sensed specific force and sensed angular velocity weights are tuned to decrease the motion sensation error with respect to the workspace boundaries of the Hexapod MSP for MPC-based MCA without using fuzzy logic. Also, weights of inputs and inputs variation of MPC-based MCA using fuzzy logic are employed similar to MPC-based MCA without using fuzzy logic to reach the fare comparison between them. In addition, the appropriate scale factors are chosen for the input signals to respect the MSP workspace boundaries (Table I). The tuning indexes of the current and proposed MPC-based MCAs are shown in Table V. In addition, the SimMechanic model of the Hexapod MSP [47] is developed to cogitate the physical and dynamical constraints of the Hexapod model as close as possible to the real one.

The Rigs of Rods (RoR) application (version 0.39.5) is used to record a driving scenario in the longitudinal channel for 35 seconds, as presented in Fig. 8.a-b. Fig. 8.a presents the linear acceleration signal along the *x*-axis, and Fig. 8.b peresents the angular velocity signal along *pitch*-angle. The scale factor of the linear acceleration and angular velocity is defined to be 0.5 and 0.2, respectively, to respect the MSP workspace boundaries. The same scale factors are employed for classical

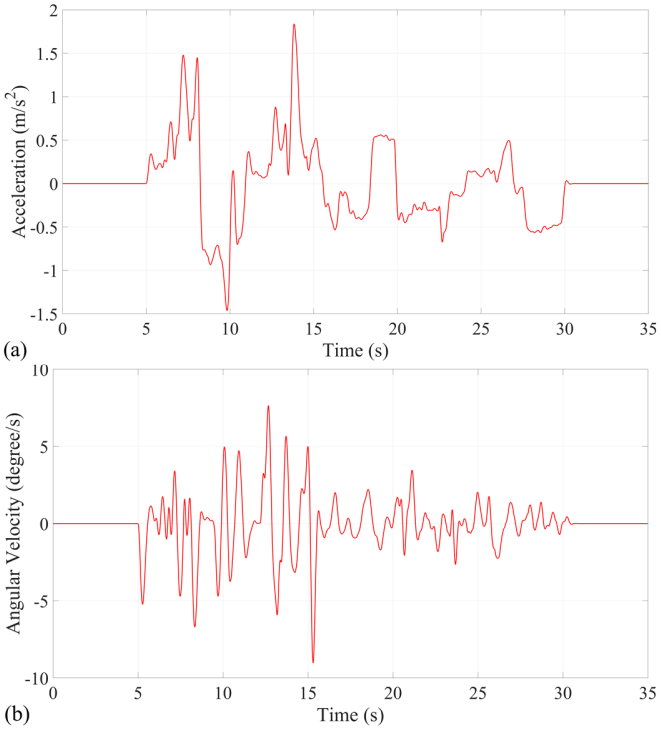


Fig. 8. The real vehicle motion signals: (a) linear acceleration; (b) angular velocity.

TABLE V
The Initial Indexes of the Current and Proposed MPC-based MCAs

Index	Current MPC	Proposed MPC
Scale factor of a_x	1/4	1/4
Scale factor of $\dot{\theta}$	1/2	1/2
N_P	150	150
N_c	3	3
Weight of $\hat{f}_x$	1000	1000
Weight of x	1600	700-2500
Weight of V_x	12.5	5-20
Weight of a_x	0.0001	0.0001
Weight of $Jerk_x$	1	1
Weight of $\hat{\theta}$	6500	6500
Weight of θ	225	50-400
Weight of $\dot{\theta}$	0.1	0.1
Weight of $\ddot{\theta}$	1	1

a_x: linear acceleration; a_x: angular velocity; N_p: prediction horizon; N_c: control horizon; $\hat{f}_x$: sensed spicific force; x: linear displacement; V_x: linear velocity; a_x: linear acceleration; $Jerk_x$: linear jerk; $\hat{\theta}$: sensed angular velocity; θ: angular dispalcement; $\dot{\theta}$: angular velocity; $\ddot{\theta}$: angular acceleration;

TABLE VI
The Result for the Classical Washout Filter, Proposed and Current MPC-based MCAs

Index	RMSE Cl WF	RMSE Ex MPC	RMSE Pr MPC	CC Cl WF	CC Ex MPC	CC Pr MPC
SCC pitch-dot	0.0339	0.0339	0.0279	0.2140	0.3527	0.6338
OTO ax	0.4425	0.3844	0.3358	0.1766	0.4606	0.6596

RMSE: Root Mean Square Error; CC: Correlation Coefficient; Cl: Classical; Ex: Existing; OTO: Otolith Organ; Pr: Proposed; SCC: Semicircular System; WF: Washout Filter.

washout filter and both proposed and current MPC-based MCAs to reach the proper comparison between three methods [62, 63].

Table VI shows the results of classical washout filter, current and proposed MPC-based MCAs. The absolute motion feeling error between the real car and MSP users is represented using a RMSE. Using the proposed method, the RMSE of sensed angular velocity along the longitudinal channel decreases by 17.94% and 17.69% as compared with those the classical washout filter and current MPC-based MCA. Similarly, the proposed method can improve the RMSE of sensed specific force along the longitudinal channel decreases by 29.73% and 12.64% as compared with those from the classical washout filter and current MPC-based MCA, respectively. The proposed method is able to reduce the RMSE of sensed specific force along the longitudinal channel from 0.3844 to 0.3358. This is an important achievement because the proposed method is able to reduce the sensed specific force error without any negative impact on the sensed angular velocity. Asadi et al. [1, 11] introduced the use of CC for evaluating the MCA in term of the shape similarity pertaining to the sensed motion signals between the real car and MSP users. As the human vestibular system cannot perceive the quantitative measure of the motion signal, this shape similarity of the regenerated motion signal is useful to ascertain the improvement of the MCA objectively. The CC metric indicates improvements of 79.70% and 43.20% corresponding to the rotational and translational motion sensation, respectively using the proposed MPC-based MCA, as compared with those of current MPC-based MCA models. This observation positively indicate that the proposed method outperforms the previous method with a large margin of improvement in the shape similarity measure.

Fig. 9.a-b represent the sensed specific force and the sensed angular velocity along the *x*-axis and *pitch*-angle for the real car and MSP users using the classical washout filter and MPC-based MCAs with and without using fuzzy logic during the recorded motion scenario. Fig. 9.a illustrates the better regeneration of the sensed angular velocity for the MSP user using the proposed MPC-based MCA compared with classical washout filter and current MPC-based MCA due to the higher CC. Also, Fig. 9.b presents the sensed specific force by the real car and MSP using three proposed methods. The sensed specific force signal follows the real vehicle user's sensed specific force using the proposed MPC because of the wise utilization of the workspace limitation compared with classical washout filter and current MPC-based MCA using constant weighting parameters.

Fig. 10.a presents the error of the sensed angular velocity along the *pitch*-angle between the real car and MSP users by the classical washout filter and MPC-based MCAs with and without fuzzy. The maximum error rates of sensed angular velocity from the classical washout filter as well as the current and proposed MPC-based MCA models are 0.0871, 0.1218, and 0.0991 rad/s, respectively. The proposed MPC-based MCA can decrease the error of the sensed angular velocity along the *pitch*-angle by considering the sensed angular velocity error and online position of the cockpit in the fuzzy logic controller.

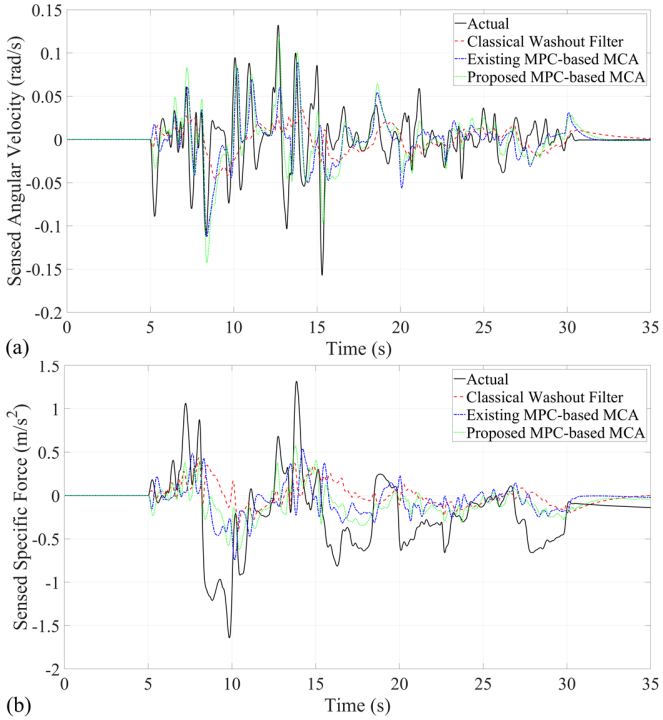


Fig. 9. The sensed angular velocity and specific force for the classical washout filter, current and proposed MPC-based MCAs along: (a) *pitch*-angle; (b) *x*-axis.

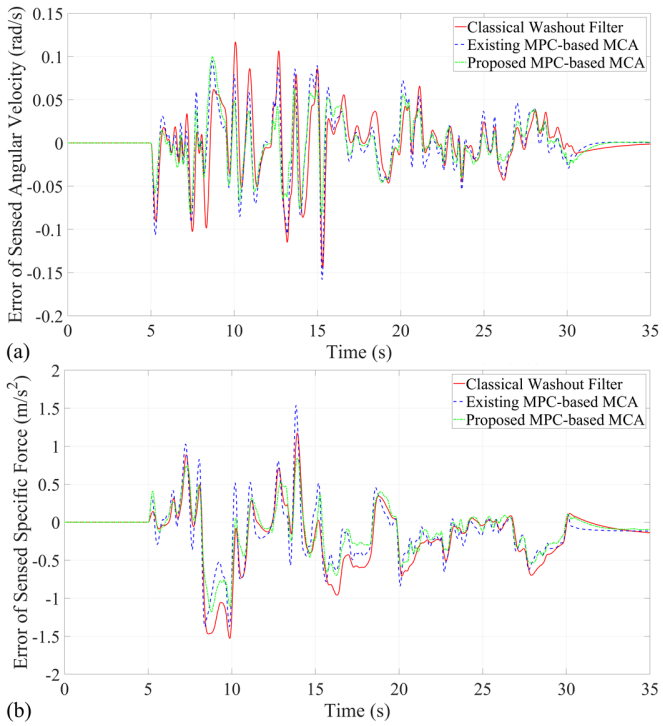


Fig. 10. The sensed angular velocity and sensed specific force errors for the classical washout filter, current and proposed MPC-based MCAs along: (a) *pitch*-angle; (b) *x*-axis.

Based on Fig. 10.b, the maximum error rates of sensed specific force along the longitudinal channel from the classical washout filter as well as the current MPC-based MCA (with constant

weighting parameters) and proposed MPC-based MCA (with time-varying weighting parameters) are 1.0262, 1.4852, and 0.9353 m/s^2, respectively. This reduction in the sensed specific force error using the proposed MPC-based MCA proves that the proposed method is more effective than the classical washout filter and current MPC-based MCA.

Fig. 11.a-b present the angular and linear displacement of the Hexapod platform using classical washout filter and MPC-based MCA with and without using fuzzy logic. The proposed method uses the more workspace area while respecting the workspace limitation.

The results demonstrate that proposed time-varying weight MPC-based MCA can reproduce the accurate motion signal for the MSP user with less false motion cues. It can consider the current position of the manipulator and current situation of the motion signals and accordingly use the platform's workspace more efficiently.

V. Conclusion

MPC-based MCA has introduced to consider the limitations of MSP. The current MPC-based MCAs have constant weights that cause the conservative utilization of the platform's workspace they should respect to the workspace limitations. They are not able to consider the current position of the cockpit and motion scenario to reproduce weights of MPC. Then, they should be tunned based on worst case scenario to respect the workspace boundaries of the MSP. While this assumption increases the motion sensation error for the user of the MSP in different driving scenarios. The MPC-based MCA using fuzzy logic to adaptively vary the output weights of the model is proposed in this study to consider the motion sensation error between the real car and MSP users as well as the current motion status of the MSP including linear position, linear velocity and angular position. In other words, the proposed MCA exploits the current position of the cockpit and motion sensation error to penalize the cockpit and ensure that the workspace constraints are satisfied, or to regenerate a large motion signal when the cockpit is close to the neutral position. This aims to better use the workspace of the MSP without imposing conservative motions. The method for varying the weighting parameters through the fuzzy controller to improve the capability of the MPC-based MCA is proposed for the first time in this paper. The membership functions of the fuzzy logic units are tuned with a multi-objective genetic algorithm, in order to increase the efficiency of the proposed method. In addition, the compensator unit is added to the model for updating the fuzzy control action based on the position and moving direction of the cockpit. For evaluation, the classical washout filter as well as the current and proposed MPC-based MCA models are designed using the MATLAB. The outcomes obtained ascertain the efficiency of the proposed method for adaptive weight tuning, as it is able to improve the motion fidelity for the MSP user. Based on the proposed model, the MSP is able to better utilize the workspace. The method imposes penalty to the motion when the cockpit is close to the workspace boundaries. The subjective study of the proposed method can be conducted as a future work to show the higher capability of the method. It should be noted that this was out of our hand due to the difficulty of human subjective evaluation during COVID19 situation and restrictions in conducting any subjective testing by Australian universities.

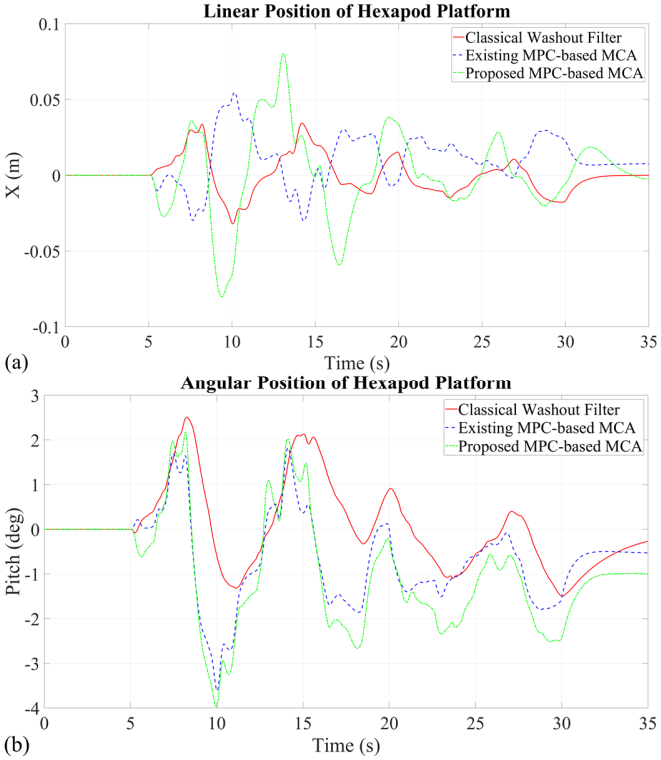


Fig. 11. The linear and angular displacement of Hexapod MSP for the classical washout filter, current and proposed MPC-based MCAs along: (a) *x*-axis; (b) *Pitch*-angle.

Acknowledgment

This research was conducted by the **Australian Research Council Centre of Excellence/ARC Special Research Centre/ ARC Key Centre for DE210101623** and funded by the Australian Government.

References

[1] H. Asadi, S. Mohamed, C. P. Lim, and S. Nahavandi, "Robust optimal motion cueing algorithm based on the linear quadratic regulator method and a genetic algorithm," *IEEE Transactions on Systems, Man, and Cybernetics: Systems,* vol. 47, no. 2, pp. 238-254, 2016.

[2] M. R. C. Qazani, H. Asadi, S. Mohamed, and S. Nahavandi, "Prepositioning of a Land Vehicle Simulation-Based Motion Platform Using Fuzzy Logic and Neural Network," *IEEE Transactions on Vehicular Technology,* vol. 69, no. 10, pp. 10446-10456, 2020.

[3] T. Tettamanti, A. Mohammadi, H. Asadi, and I. Varga, "A two-level urban traffic control for autonomous vehicles to improve network-wide performance," *Transportation research procedia,* vol. 27, pp. 913-920, 2017.

[4] J.-P. Merlet, *Parallel robots*. Springer Science & Business Media, 2006.

[5] M. R. C. Qazani, H. Asadi, and S. Nahavandi, "High-fidelity hexarot simulation-based motion platform using fuzzy incremental controller and model predictive control-based motion cueing algorithm," *IEEE Systems Journal,* vol. 14, no. 4, pp. 5073-5083, 2019.

[6] M. R. C. Qazani, H. Asadi, and S. Nahavandi, "A new gantry-tau-based mechanism using spherical wrist and model predictive

control-based motion cueing algorithm," *Robotica,* vol. 38, no. 8, pp. 1359-1380, 2020.

[7] H. Asadi, "Human perception-based washout filtering," Deakin University, 2015.

[8] B. Conrad and S. F. Schmidt, "A study of techniques for calculating motion drive signals for flight simulators," 1971.

[9] H. Asadi, S. Mohamed, K. Nelson, S. Nahavandi, and D. R. Zadeh, "Human perception-based washout filtering using genetic algorithm," in *International Conference on Neural Information Processing*, 2015: Springer, pp. 401-411.

[10] S. F. Schmidt, *Motion drive signals for piloted flight simulators*. National Aeronautics and Space Administration, 1970.

[11] H. Asadi, S. Mohamed, and S. Nahavandi, "Incorporating human perception with the motion washout filter using fuzzy logic control," *IEEE/ASME Transactions on Mechatronics,* vol. 20, no. 6, pp. 3276-3284, 2015.

[12] H. Asadi, A. Mohammadi, C. P. Lim, S. Mohamed, D. Nahavandi, and S. Nahavandi, "Increasing Motion Fidelity in Driving Simulators Using a Fuzzy-Based Washout Filter," *IEEE Transactions on Intelligent Vehicles,* 2019.

[13] M. R. C. Qazani, H. Asadi, T. Bellmann, S. Mohamed, C. P. Lim, and S. Nahavandi, "Adaptive Washout Filter Based on Fuzzy Logic for a Motion Simulation Platform With Consideration of Joints' Limitations," *IEEE Transactions on Vehicular Technology,* vol. 69, no. 11, pp. 12547-12558, 2020.

[14] M. R. C. Qazani, H. Asadi, T. Bellmann, S. Perdrammehr, S. Mohamed, and S. Nahavandi, "A New Fuzzy Logic Based Adaptive Motion Cueing Algorithm Using Parallel Simulation-Based Motion Platform," in *2020 IEEE International Conference on Fuzzy Systems (FUZZ-IEEE)*, 2020: IEEE, pp. 1-8.

[15] M. R. C. Qazani, H. Asadi, M. Rostami, S. Mohamed, C. P. Lim, and S. Nahavandi, "Adaptive Motion Cueing Algorithm Based on Fuzzy Logic Using Online Dexterity and Direction Monitoring," *IEEE Systems Journal,* 2021.

[16] H. Asadi, S. Mohamed, K. Nelson, and S. Nahavandi, "A linear quadratic optimal motion cueing algorithm based on human perception," in *ACRA 2014: Proceedings of Australasian Conference on Robotics and Automation*, 2014: Australian Robotics and Automation Association, pp. 1-9.

[17] R. J. Telban and F. M. Cardullo, "Motion cueing algorithm development: Human-centered linear and nonlinear approaches," *NASA TechReport CR-2005-213747,* 2005.

[18] H. Asadi, S. Mohamed, K. Nelson, S. Nahavandi, and M. Oladazimi, "An optimal washout filter based on genetic algorithm compensators for improving simulator driver perception," in *DSC 2015: Proceedings of the Driving Simulation Conference & Exhibition*, 2015: Max Planck Institute for the Advancement of Science, pp. 1-10.

[19] H. Asadi, S. Mohamed, D. Rahim Zadeh, and S. Nahavandi, "Optimisation of nonlinear motion cueing algorithm based on genetic algorithm," *Vehicle System Dynamics,* vol. 53, no. 4, pp. 526-545, 2015.

[20] M. R. C. Qazani, H. Asadi, and S. Nahavandi, "An Optimal Motion Cueing Algorithm Using the Inverse Kinematic solution of the Hexapod Simulation Platform," *IEEE Transactions on Intelligent Vehicles,* 2021.

[21] M. Dagdelen, G. Reymond, A. Kemeny, M. Bordier, and N. Maïzi, "Model-based predictive motion cueing strategy for vehicle driving simulators," *Control Engineering Practice,* vol. 17, no. 9, pp. 995-1003, 2009.

[22] Z. Fang and A. Kemeny, "Explicit MPC motion cueing algorithm for real-time driving simulator," in *Proceedings of The 7th International Power Electronics and Motion Control Conference*, 2012, vol. 2: IEEE, pp. 874-878.

[23] A. Mohammadi, H. Asadi, S. Mohamed, K. Nelson, and S. Nahavandi, "MPC-based motion cueing algorithm with short prediction horizon using exponential weighting," in *2016 IEEE International Conference on Systems, Man, and Cybernetics (SMC)*, 2016: IEEE, pp. 000521-000526.

[24] M. Bruschetta, F. Maran, and A. Beghi, "A fast implementation of mpc-based motion cueing algorithms for mid-size road vehicle motion simulators," *Vehicle system dynamics,* vol. 55, no. 6, pp. 802-826, 2017.

[25] A. Mohammadi, H. Asadi, S. Mohamed, K. Nelson, and S. Nahavandi, "Multiobjective and interactive genetic algorithms for weight tuning of a model predictive control-based motion cueing algorithm," *IEEE transactions on cybernetics,* vol. 49, no. 9, pp. 3471-3481, 2018.

[26] M. R. C. Qazani, H. Asadi, and S. Nahavandi, "A decoupled linear model predictive control-based motion cueing algorithm for simulation-based motion platform with limitted workspace," in *IEEE International Conference on Systems, Man, and Cybernetics (SMC), Bari, Italy*, 2019, pp. 1-6.

[27] M. R. C. Qazani, H. Asadi, S. Khoo, and S. Nahavandi, "A Linear Time-Varying Model Predictive Control-Based Motion Cueing Algorithm for Hexapod Simulation-Based Motion Platform," *IEEE Transactions on Systems, Man, and Cybernetic: Systems,* 2019, doi: 10.1109/TSMC.2019.2958062.

[28] M. R. C. Qazani, H. Asadi, and S. Nahavandi, "A Model Predictive Control-Based Motion Cueing Algorithm with Consideration of Joints' limitations for Hexapod Motion Platform," in *2019 IEEE International Conference on Systems, Man and Cybernetics (SMC)*, 2019: IEEE, pp. 708-713.

[29] T. Miunske, J. Pradipta, and O. Sawodny, "Model Predictive Motion Cueing Algorithm for an Overdetermined Stewart Platform," *Journal of Dynamic Systems, Measurement, and Control,* vol. 141, no. 2, 2019.

[30] M. Grottoli, D. Cleij, P. Pretto, Y. Lemmens, R. Happee, and H. H. Bülthoff, "Objective evaluation of prediction strategies for optimization-based motion cueing," *Simulation,* vol. 95, no. 8, pp. 707-724, 2019.

[31] S. Casas-Yrurzum, C. Portalés-Ricart, P. Morillo-Tena, and C. Cruz-Neira, "On the Objective Evaluation of Motion Cueing in Vehicle Simulations," *IEEE Transactions on Intelligent Transportation Systems,* 2020.

[32] S. Casas, C. Portalés, P. Morillo, and M. Fernández, "To move or not to move? Analyzing motion cueing in vehicle simulators by means of massive simulations," *Virtual Reality,* vol. 24, no. 1, pp. 93-108, 2020.

[33] D. Arjoni *et al.*, "Experimental Evaluation of the Human Performance on a RoboticFlight Simulator based on FOQA Parameters," in *Aerospace Technology Conference 2016, Swedish Aerospace Technology in a Globalised World, October 11-12, Solna, Stockholm, Sweden*, 2016, vol. 1, pp. 1-11.

[34] G. S. Natal *et al.*, "Implementation analysis of a washout filter on a robotic flight simulator-A case study," *Journal of Aerospace Technology and Management,* vol. 11, 2019.

[35] M. A. Pieters, P. Zaal, D. M. Pool, O. Stroosma, and M. Mulder, "A Simulator Comparison Study into the Effects of Motion Filter Order on Pilot Control Behavior," in *AIAA Scitech 2019 Forum*, 2019, p. 0712.

[36] E. N. Bachelder and M. Godfroy-Cooper, "Pilot Workload Estimation: Synthesis of Spectral Requirements Analysis and Weber's Law," in *AIAA Scitech 2019 Forum*, 2019, p. 1228.

[37] M. Katliar, F. M. Drop, H. Teufell, M. Diehl, and H. H. Bülthoff, "Real-Time Nonlinear Model Predictive Control of a Motion Simulator Based on a 8-DOF Serial Robot," in *2018 European Control Conference (ECC)*, 2018: IEEE, pp. 1529-1535.

[38] E. F. Camacho and C. B. Alba, *Model predictive control*. Springer Science & Business Media, 2013.

[39] K. I. Kouramas, N. P. Faísca, C. Panos, and E. N. Pistikopoulos, "Explicit/multi-parametric model predictive control (MPC) of linear discrete-time systems by dynamic and multi-parametric programming," *Automatica,* vol. 47, no. 8, pp. 1638-1645, 2011.

[40] S. Casas, C. Portales, J. Gimeno, and M. Fernandez, "Simulation of parallel mechanisms for motion cueing generation in vehicle simulators using AM-FM bi-modulated signals," *Mechatronics,* vol. 53, pp. 251-261, 2018.

[41] S. Pedrammehr, M. R. C. Qazani, H. Asadi, and S. Nahavandi, "Kinematic Manipulability Analysis of Hexarot Simulators," in *ICIT*, 2019, pp. 133-138.

[42] S. Pedrammehr, M. R. C. Qazani, H. Asadi, and S. Nahavandi, "Control System Development of a Hexarot-Based High-G Centrifugal Simulator," in *ICIT*, 2019, pp. 78-83.

[43] S. Pedrammehr, H. Asadi, and S. Nahavandi, "The forced vibration analysis of hexarot parallel mechanisms," in *2019 IEEE International Conference on Industrial Technology (ICIT)*, 2019: IEEE, pp. 199-204.

[44] S. Pedrammehr, M. R. C. Qazani, H. Asadi, and S. Nahavandi, "Manipulability Analysis of Gantry-Tau parallel manipulator," in

ACRA 2019: Proceedings of the Australasian Conference on Robotics and Automation, 2019: [Australian Robotics & Automation Association], pp. 1-7.

[45] M. R. C. Qazani, V. Mohammadi, H. Asadi, S. Mohamed, and S. Nahavandi, "Development of Gantry-Tau-3R Mechanism Using a Neuro PID Controller," in *ACRA 2019: Proceedings of the Australasian Conference on Robotics and Automation*, 2019: [Australian Robotics & Automation Association], pp. 1-8.

[46] M. R. C. Qazani, S. Pedrammehr, H. Abdi, and S. Nahavandi, "Performance evaluation and calibration of gantry-tau parallel mechanism," *Iranian Journal of Science and Technology, Transactions of Mechanical Engineering,* pp. 1-15, 2019.

[47] M. R. C. Qazani, S. Pedrammehr, and M. J. Nategh, "An investigation on the motion error of machine tools' hexapod table," *International Journal of Precision Engineering and Manufacturing,* vol. 19, no. 4, pp. 463-471, 2018.

[48] M. R. C. Qazani, H. Asadi, S. Pedrammehr, and S. Nahavandi, "Performance analysis and dexterity monitoring of hexapod-based simulator," in *2018 4th International Conference on Control, Automation and Robotics (ICCAR)*, 2018: IEEE, pp. 226-231.

[49] H. Asadi, S. Mohamed, C. P. Lim, and S. Nahavandi, "A review on otolith models in human perception," *Behavioural brain research,* vol. 309, pp. 67-76, 2016.

[50] H. Asadi, S. Mohamed, C. P. Lim, S. Nahavandi, and E. Nalivaiko, "Semicircular canal modeling in human perception," *Reviews in the Neurosciences,* vol. 28, no. 5, pp. 537-549, 2017.

[51] A. Mohammadi, H. Asadi, S. Mohamed, K. Nelson, and S. Nahavandi, "Optimizing model predictive control horizons using genetic algorithm for motion cueing algorithm," *Expert Systems with Applications,* vol. 92, pp. 73-81, 2018.

[52] M. R. C. Qazani, S. M. J. Jalali, H. Asadi, and S. Nahavandi, "Optimising Control and Prediction Horizons of a Model Predictive Control-Based Motion Cueing Algorithm Using Butterfly Optimization Algorithm," in *2020 IEEE Congress on Evolutionary Computation (CEC)*, 2020: IEEE, pp. 1-8.

[53] R. R. Yager and L. A. Zadeh, *An introduction to fuzzy logic applications in intelligent systems*. Springer Science & Business Media, 2012.

[54] K. Yuan, Q. Wang, and L. Wang, "Fuzzy-logic-based terrain identification with multisensor fusion for transtibial amputees," *IEEE/ASME Transactions on Mechatronics,* vol. 20, no. 2, pp. 618-630, 2015.

[55] H. Asadi, S. Kaboli, M. Oladazimi, and M. Safari, "A review on Li-ion battery charger techniques and optimize battery charger performance by fuzzy logic," *ICICA,* vol. 18, no. 201, pp. 89-96, 2011.

[56] D. Kalyanmoy, *Multi objective optimization using evolutionary algorithms*. John Wiley and Sons, 2001.

[57] A. Mohammadi, H. Asadi, S. Mohamed, K. Nelson, and S. Nahavandi, "OpenGA, a C++ genetic algorithm library," in *2017 IEEE International Conference on Systems, Man, and Cybernetics (SMC)*, 2017: IEEE, pp. 2051-2056.

[58] K. A. De Jong, "Analysis of the behavior of a class of genetic adaptive systems," 1975.

[59] M. Mitchell, *An introduction to genetic algorithms*. MIT press, 1998.

[60] E. Pellerin, L. Pigeon, and S. Delisle, "Self-adaptive parameters in genetic algorithms," in *Data Mining and Knowledge Discovery: Theory, Tools, and Technology VI*, 2004, vol. 5433: International Society for Optics and Photonics, pp. 53-65.

[61] C. Schmid and L. T. Biegler, "Quadratic programming methods for reduced hessian SQP," *Computers & chemical engineering,* vol. 18, no. 9, pp. 817-832, 1994.

[62] H. Asadi, C. P. Lim, A. Mohammadi, S. Mohamed, S. Nahavandi, and L. Shanmugam, "A genetic algorithm–based nonlinear scaling method for optimal motion cueing algorithm in driving simulator," *Proceedings of the Institution of Mechanical Engineers, Part I: Journal of Systems and Control Engineering,* vol. 232, no. 8, pp. 1025-1038, 2018.

[63] H. Asadi *et al.*, "A Model Predictive Control-based Motion Cueing Algorithm using an optimized Nonlinear Scaling for Driving Simulators," in *2019 IEEE International Conference on Systems, Man and Cybernetics (SMC)*, 2019: IEEE, pp. 1245-1250.



Mohammad Reza Chalak Qazani received the Bachelor of Engineering in manufacturing and production from University of Tabriz, Tabriz, Iran in 2010 and the master's degree in robotic and mechanical engineering from the Tarbiat Modares University, Tehran, Iran, in 2013. He received the Ph.D. degree in modelling and simulation of a motion cueing algorithm using prediction and computational intelligence techniques from the Institute for Intelligent Systems Research and Innovation (IISRI), Deakin University, Australia, in 2021.

He is currently an Alfred Deakin Postdoctoral Research Fellow in the Institute for Intelligent Systems Research and Innovation (IISRI), Deakin University. His current research interests include model predictive control, motion cueing algorithm and soft computing controllers.



Houshyar Asadi received the Bachelor of Engineering degree (First Class Hons.) in electrical-control systems in 2008, and master's degree in industrial Electronic and Control Engineering from University of Malaya in 2012. He received the Ph.D. degree in human perception-based washout filtering using Artificial intelligence (AI) from the Institute for Intelligent Systems Research and Innovation (IISRI), Deakin University, Australia, in 2015.

He is currently a Senior Research Fellow of Control and Motion Analysis with the IISRI, Deakin University. His current research interests include computational intelligence, motion-based simulator technologies, motion cueing algorithms, robotics, control, and human factors in virtual environments.



Shady Mohamed received the B.Sc. and M.Sc. degrees in information technology from Cairo University, Giza, Egypt, in 2000 and 2003, respectively, and the Ph.D. degree in control theory from Deakin University, Geelong, VIC, Australia, in 2009. He is currently an associated professor with the Institute for Intelligent Systems Research and Innovation (IISRI), Deakin University, Australia.

He is interested in interdisciplinary research involving signal processing, control theory, human biodynamics, haptics and medical imaging.



Chee Peng Lim received his PhD degree from the University of Sheffield, UK, in 1997. His research interests include computational intelligence-based systems for pattern recognition, data mining, fault detection, condition monitoring, decision support, and process optimization. He has published over 481 technical papers in these areas.

He is currently a professor at Institute for Intelligent Systems Research and Innovation, Deakin University, Australia.



Saeid Nahavandi received a Ph.D. from Durham University, U.K. in 1991. He is an Alfred Deakin Professor, Pro Vice-Chancellor, Chair of Engineering, and the Founding Director of the Institute for Intelligent Systems Research and Innovation at Deakin University. His research interests include modelling of complex systems, robotics and haptics. He has published over 900 scientific papers in various international journals and conferences.

Professor Nahavandi is Editor-In-Chief: IEEE SMC Magazine, the Senior Associate Editor: IEEE Systems Journal, Associate Editor of IEEE Transactions on Systems, Man and Cybernetics: Systems, and IEEE Press Editorial Board member. Professor Nahavandi is a Fellow of IEEE (FIEEE), Engineers Australia (FIEAust), the Institution of Engineering and Technology (FIET). Saeid is a Fellow of the Australian Academy of Technology and Engineering (ATSE).